

## Efficient Degradation of Toxic Organic Pollutants with $\text{Ni}_2\text{O}_3/\text{TiO}_2-x\text{B}_x$ under Visible Irradiation

Wei Zhao,<sup>†</sup> Wanhong Ma,<sup>†</sup> Chuncheng Chen,<sup>†</sup> Jincal Zhao,<sup>\*,†</sup> and Zhigang Shuai<sup>‡</sup>  
Key Laboratory of Photochemistry and Key Laboratory of Organic Solids, Institute of Chemistry,  
Chinese Academy of Sciences, Beijing 100080, China

Received November 19, 2003; E-mail: jczhao@iccas.ac.cn

Since  $\text{TiO}_2$  was found to be an efficient photocatalyst,<sup>1</sup> intense research has concentrated on anatase  $\text{TiO}_2$  photocatalysis. However, this material is only active upon UV excitation because of its large energy band gap of 3.2 eV. Recently, doping  $\text{TiO}_2$  with nonmetal atoms has received a lot of attention.<sup>2–6</sup> For example, Asahi et al.<sup>2</sup> and Khan et al.<sup>3</sup> reported that doping  $\text{TiO}_2$  with nitrogen or carbon can lower its band gap and shift its optical response to the visible region. Here we report on doped  $\text{TiO}_2$  with both a nonmetal element, boron, and a metal oxide,  $\text{Ni}_2\text{O}_3$ , by a simple method of modified sol–gel synthesis.<sup>7</sup> Our findings suggest that incorporation of B into  $\text{TiO}_2$  can extend the spectral response to the visible region and that the photocatalytic activity is greatly enhanced as it is further loaded with  $\text{Ni}_2\text{O}_3$ . The goals both of extending the  $\text{TiO}_2$  spectral response to the visible region and of improving its catalytic activity are realized by modification with two dopants, the nonmetal and metal oxide.

Because the dyes can be easily degraded in aqueous pure  $\text{TiO}_2$  dispersion under visible irradiation as we reported before,<sup>8</sup> here we chose trichlorophenol (TCP), 2,4-dichlorophenol (2,4-DCP), and sodium benzoate which have no absorption in the visible region as the target pollutants. A halogen lamp was used as the light source, and it was equipped with a cutoff filter to completely remove any radiation below 420 nm and to ensure illumination by visible light only. Though all the samples exhibit high photocatalytic activity under UV irradiation, the data displayed in Figure 1A clearly indicate that under otherwise identical conditions a boron- and nickel-doped titania photocatalyst exhibits much greater activity than pure  $\text{TiO}_2$  or  $\text{TiO}_2$  doped with only boron or only nickel oxide in the visible region, although a solely boron-doped catalyst also exhibits some activity. In the degradation process in the boron- and nickel-doped titania system, about 80% of the total chloride content is converted into  $\text{Cl}^-$  ions after illumination for 4 h (Figure 1B). A reduction of about 80%  $\text{COD}_{\text{Cr}}$  value and 70% of total organic carbon (TOC) were also achieved, indicating that TCP had been not only degraded but also mineralized efficiently under visible light irradiation. Furthermore, the efficient degradation of 2,4-DCP and sodium benzoate on the boron- and nickel-doped titania catalyst under visible light irradiation was also observed similar to that of TCP.

Figure 2 gives the UV–vis diffuse reflectance absorption spectra of the pure  $\text{TiO}_2$  and doped  $\text{TiO}_2$  samples. Compared to pure  $\text{TiO}_2$ , the absorption of boron-doped sample extends significantly into the visible region. It is clear that the incorporation of boron results in a substantial red-shift of the absorption of  $\text{TiO}_2$  material. Compared to that of boron-doped titania, the absorption of the sample doped with both nickel and boron exhibits somewhat of a red-shift. The plot of transformed Kubelka–Munk function versus the energy of light (Figure 2) affords band gap energies of 3.18, 2.93, and 2.85 eV for pure  $\text{TiO}_2$ , boron-doped  $\text{TiO}_2$ , and boron-

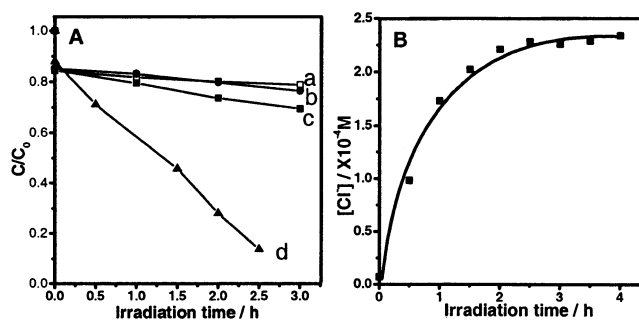


**Figure 1.** (A) Temporal course of the photodegradation of TCP ( $1.0 \times 10^{-4}$  M; 50 mL) in aqueous dispersions containing 50 mg of catalysts under visible light irradiation: (a) pure  $\text{TiO}_2$ , (b) nickel-doped  $\text{TiO}_2$ , (c) boron-doped  $\text{TiO}_2$ , and (d) boron- and nickel-doped  $\text{TiO}_2$ . (B) Formation of  $\text{Cl}^-$  during the degradation process in the boron- and nickel-doped  $\text{TiO}_2$  system.

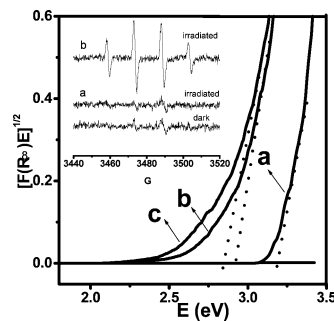


**Figure 2.** Diffuse reflectance absorption spectra of (a) pure  $\text{TiO}_2$ , (b) boron-doped  $\text{TiO}_2$ , and (c) boron- and nickel-doped  $\text{TiO}_2$ . Data are plotted as transformed Kubelka–Munk function versus the energy of light. Inset showing changes of ESR signal of the  $\text{DMPO}-\cdot\text{OH}$  adducts in the suspensions of (a) P25 and (b) boron- and nickel-doped  $\text{TiO}_2$  before and after irradiation.

and nickel-doped  $\text{TiO}_2$ , respectively. Accordingly, this absorption feature suggests that the photocatalyst can possibly be activated by visible light.

We employed the ESR spin-trap technique (with DMPO) to probe the nature of the reactive oxygen species generated on the surface of catalysts under visible irradiation.<sup>9</sup> A Nd:YAG laser ( $\lambda = 532$  nm) was employed to irradiate suspensions containing catalysts. Very weak  $\text{DMPO}-\cdot\text{OH}$  signals were detected in the irradiated suspension of titania doped only with boron. However, as depicted in the insert of Figure 2, four characteristic peaks of  $\text{DMPO}-\cdot\text{OH}$  were obviously observed in the suspension of titania doped with both boron and nickel, and their intensity increased with irradiation time. No such signals were detected in the dark. This means that irradiation is essential to the generation of  $\cdot\text{OH}$  on the surface of the catalyst. In contrast, no  $\cdot\text{OH}$  signals were detected in either pure  $\text{TiO}_2$  or only nickel-doped  $\text{TiO}_2$  systems under the otherwise identical conditions. Though visible light-induced polymerization of TCP can occur on P25  $\text{TiO}_2$ ,<sup>10</sup> this

<sup>†</sup> Key Laboratory of Photochemistry.

<sup>‡</sup> Key Laboratory of Organic Solids.

process could not result in dechlorination and mineralization since P25 cannot be excited by visible light. Similarly, the  $\text{DMPO-O}_2^{\cdot-}$  species were detected successfully in the boron- and nickel-doped titania suspension under visible light irradiation. The evidence that  $\cdot\text{OH}$  and  $\text{O}_2^{\cdot-}$  are produced on the surface of visible illuminated boron- and nickel-doped titania provides a solid indication that the catalyst can be efficiently excited by visible light to create electron-hole pairs and that the charge separation is maintained long enough to react with adsorbed oxygen/ $\text{H}_2\text{O}$  and to produce a series of active oxygen radicals which finally induce the decomposition of organic compounds as illustrated in previous work.<sup>11</sup>

X-ray diffraction analysis showed that a structure composed only of anatase formed after calcination and that there was no observable structural difference between pure  $\text{TiO}_2$  and boron-only-modified  $\text{TiO}_2$ . Full profile structure refinement of XRD data using the Rietveld program MULTI-PATTERN showed that the lattice parameters of the pure  $\text{TiO}_2$  structure were  $a = b = 3.7833(2)$  and  $c = 9.4996(3)$ , and those of the boron-modified titania structure were  $a = b = 3.7842(1)$  and  $c = 9.4549(7)$ . It is clear that the lattice parameters remain almost unchanged along the  $a$ - and  $b$ -axes while the  $c$ -axis parameter decreases as boron is doped. The existence of Ni has no impact on the crystal structure of titania doped with boron, indicating that Ni is not weaved into the crystal structure of the sample and is separated from the phase. However, because of the trace amount of Ni, no such separate phase was detected.

Determination of the oxidation state of the doped nickel was carried out by measuring Ni  $2p_{3/2}$  binding energy (BE) with X-ray photoelectron spectroscopy (XPS). The BE 855.5 eV was assigned to  $\text{Ni}_2\text{O}_3$ . No evidence of other oxidation states of nickel was found. There was no difference between the peaks of the sample before and after the catalytic reaction, indicating that the oxidation state of nickel remained stable in the reaction process. The XPS analysis also showed the presence of boron (BE 191.6 eV). To determine the oxidation state of the boron dopant, pure samples of boric acid,  $\text{B}_2\text{O}_3$ , and  $\text{TiB}_2$  were selected as standards for the XPS measurements. The results indicated that the binding energy for B1s is 194.1 eV in  $\text{B}_2\text{O}_3$  (B–O bonds) and 188.2 eV in  $\text{TiB}_2$  (Ti–B bonds). The XPS results display that the boron atom was incorporated into  $\text{TiO}_2$  rather than existing in a separate phase of  $\text{B}_2\text{O}_3$  or  $\text{H}_3\text{BO}_3$  (BE 193.8 eV) and the chemical environment surrounding boron is neither B–Ti–B nor B–O. Some mixed state such as B–Ti–O (with a BE between those of  $\text{B}_2\text{O}_3$  and  $\text{TiB}_2$ ) may be the case. The boron- and nickel-doped catalyst was denoted as  $\text{Ni}_2\text{O}_3/\text{TiO}_{2-x}\text{B}_x$ . We have carried out DFT calculations for three systems: O substituted by B, Ti substituted by B, and interstitial B doping. The results show that the system of O substituted by B has the lowest energy, indicating that it is the most stable state. The theoretical densities of states (DOSs) for the O substitution case reveal that the p orbital of B is mixed with O 2p orbitals which is responsible for the band gap narrowing. However, to get more detailed solid information on the structure of the catalyst, further work is needed. A series of photocatalysts containing different concentrations of boron and nickel were prepared, and their photocatalytic activities were measured. The results showed that the catalyst containing ~1.32 atomic % for boron and ~0.68 atomic % for nickel, determined by the XPS peaks at 855.5 and 191.6 eV, respectively, was found to be the most efficient for the degradation of TCP among these samples examined. The XPS spectra of  $\text{Ti}_{2p_{3/2}}$  in  $\text{TiO}_2$  can be fitted as one peak at 458.5 eV, indicating that Ti ions are in an octahedral environment. Note that the same result was obtained in  $\text{Ni}_2\text{O}_3/\text{TiO}_{2-x}\text{B}_x$ , which ruled out the presence of  $\text{Ti}^{3+}$ . The XPS spectra of the O 1s region were also taken. The O

1s region of the pure  $\text{TiO}_2$  is composed of two peaks at 529.8 and 531.5 eV, corresponding to the Ti–O bond in  $\text{TiO}_2$  and hydroxyl groups on the surface. However, the broad O 1s region of  $\text{Ni}_2\text{O}_3/\text{TiO}_{2-x}\text{B}_x$  can be fitted by three peaks, which are Ti–O in  $\text{TiO}_2$ , Ni–O, and the surface hydroxyl groups.

The photocatalytic activity did not decrease after four successive cycles of degradation tests under visible irradiation, indicating that the incorporation of boron and nickel did not affect the stability of the catalyst.

From the above results, it seems clear that incorporation of boron atoms in  $\text{TiO}_2$  can extend the spectral response to the visible region, although its photocatalytic activity is limited. As reported by Zou et al.,<sup>12</sup> oxide nickel was shown to facilitate the excited electron transfer and hence suppress efficiently the recombination of photo-produced electron–hole. When  $\text{Ni}_2\text{O}_3$  is loaded on the surface of  $\text{TiO}_{2-x}\text{B}_x$ , the photocatalytic activity is improved efficiently since the loaded  $\text{Ni}_2\text{O}_3$  species acts as electron traps and thus facilitates the charge separation. This was suggested by the previous study on nickel oxide,<sup>12</sup> and can also be inferred from the ESR results reported in this study. In summary, this study is the first to demonstrate that the improvement of  $\text{TiO}_2$  in both spectral response and photocatalytic efficiency can be achieved through a combined approach, doping with the nonmetal boron and the metal oxide  $\text{Ni}_2\text{O}_3$ .

**Acknowledgment.** This work was supported by MSTC (No. 2003CB415006), NSFC (Nos. 20133010, 50221001, and 20371048), and CAS. We thank Dr. L. Zang (University of Southern Illinois) for his valuable discussion.

**Supporting Information Available:** COD<sub>Cr</sub>, UV–vis reflectance spectra, XPS, XRD, ESR, BET surface area, visible light degradation of TCP on different Ni, B contents of catalysts, degradation under UV irradiation, DFT calculations, and DOSs (PDF). This material is available free of charge via the Internet at <http://pubs.acs.org>.

## References

- (1) Fujishima, A.; Honda, K. *Nature* **1972**, *238*, 37.
- (2) Asahi, R.; Morikawa, T.; Ohwaki, T.; Aoki, K.; Taga, Y. *Science* **2001**, *293*, 269.
- (3) Khan, S. U. M.; Al-Shahry, M.; Ingler, W. B., Jr. *Science* **2002**, *297*, 2243.
- (4) (a) Sakthivel, S.; Kisch, H. *Angew. Chem., Int. Ed.* **2003**, *42*, 4908. (b) Sakthivel, S.; Kisch, H. *ChemPhysChem* **2003**, *4*, 487.
- (5) (a) Burda, C.; Lou, Y.; Chen, X.; Samia, A. C. S.; Stout, J.; Gole, J. L. *Nano Lett.* **2003**, *3*, 1049. (b) Umebayashi, T.; Yamaki, T.; Tanaka, S.; Asai, K. *Chem. Lett.* **2003**, *32*, 330. (c) Irie, H.; Washizuka, S.; Yoshino, N.; Hashimoto, K. *Chem. Commun.* **2003**, 1298.
- (6) (a) Irie, H.; Watanabe, Y.; Hashimoto, K. *J. Phys. Chem. B* **2003**, *107*, 5483. (b) Gole, J. L.; Stout, J. D.; Burda, C.; Lou, Y.; Chen, X. *J. Phys. Chem. B* **2004**, *108*, 1230. (c) Lindgren, T.; Mwabora, J. M.; Avendano, E.; Jonsson, J.; Hoel, A.; Granqvist, C.; Lindqvist, S. *J. Phys. Chem. B* **2003**, *107*, 5709.
- (7) A certain amount of boric acid and nickel acetate tetrahydrate was dissolved in 50 mL of methanol. Under anaerobic conditions (purged with  $\text{N}_2$ ), 2.5 mL of tetrabutyl titanate and 2.5 mL of titanous chloride were then added under vigorous magnetic stirring, and the translucent mixture was stirred for 2 h (pH value of the solution was <1). NaOH solution (1 M, 0.1 mL, every 30min) was then added slowly to the solution surrounded by ice bath for about 24 h. The clear blue solution was then stirred at room temperature for 2 days and then was turned to a water bath as it turned to a bluish milky gel. After drying, the slurry was heated to 110 °C for 200 min. Then the as-prepared sample was calcined at 400 °C for 5 h with a heating rate of 1 °C/min in nitrogen atmosphere. The yellow powders were washed repeatedly with water until no  $\text{Cl}^-$  ions were detected in the supernatant liquid. Pure  $\text{TiO}_2$  was also prepared without the addition of boric acid and nickel acetate tetrahydrate.
- (8) (a) Wu, T.; Liu, G.; Zhao, J. C.; Hidaka, H.; Serpone, N. *J. Phys. Chem. B* **1999**, *103*, 4862. (b) Wu, T.; Lin, T.; Zhao, J. C.; Hidaka, H.; Serpone, N. *Environ. Sci. Technol.* **1999**, *33*, 1379.
- (9) The ESR measurements referred to ref 8b.
- (10) Agrios, A. G.; Gray, K. A.; Weitz, E. *Langmuir* **2003**, *19*, 1402.
- (11) (a) Maldotti, A.; Molinari, A.; Amadelli, R. *Chem. Rev.* **2002**, *102*, 3811 and references therein. (b) Linsebigler, A. L.; Lu, G.; Yates, J. T., Jr. *Chem. Rev.* **1995**, *95*, 735 and references therein.
- (12) Zou, Z. G.; Ye, J. H.; Sayama, K.; Arakawa, H. *Nature* **2001**, *414*, 625.

JA0396753